LINE FORMATION IN SPHERICAL MEDIA WITH PARTIAL FREQUENCY REDISTRIBUTION

I. *Solution of the Line Transfer*

A. PERAIAH
Institut für Theoretische Astrophysik der Universität Heidelberg
and
Indian Institute of Astrophysics, Bangalore, India

(Received 3 May, 1978)

Abstract. The effects of partial redistribution of frequency on the formation of spectral lines in a static and spherically symmetric media have been investigated. The partial redistribution functions R_{I} and R_{II} (Hummer, 1962) have been employed to calculate the lines for a two-level atom in non-LTE in a spherically symmetric medium with homogeneous physical characteristics whose ratios B/A (of outer to inner radii) are equal to 2 and 10. These results are compared with those formed in a plane-parallel medium with $B/A = 1$. Two types of atmosphere are treated: (1) a pure scattering medium with $\varepsilon = 0$ and $\beta = 0$, and (2) an atmosphere with a constant source of emission $\varepsilon = 10^{-4}$ and $\beta = 0$, where ε is the probability per scatter that a photon will be destroyed by collisional de-excitation and β is the ratio K_c/K_l of opacity due to continuous absorption per unit interval of frequency to that in the line. Lines formed in complete redistribution also have been calculated for the sake of comparison, and the total optical depth in all cases has been taken to be 10^3 at the line centre.

Vast differences have been found between the lines formed by complete and partial redistribution functions (which, for the sake of simplicity, we shall hereafter refer to as CRD and PRD, respectively). In the case of a purely scattering medium, a small amount of emission is observed in the wings for all cases of scattering functions in the spherical medium as a result of the combined effects of curvature and physical scattering. In the scattering medium, more photons are scattered into the cores of the lines by PRD than in the case of CRD. The lines formed in the medium with internal sources show emission in all cases with small absorption in the cores, except those lines formed by the angle-dependent PRD functions which again depend on the geometrical extension of the medium.

1. Introduction

It is customary to use complete redistribution of frequencies in the line in calculating the transfer of line radiation from the atmospheres of stars. A considerable amount of work has been done recently on the effects of partial redistribution on the formation of spectral lines. Hummer (1969), Avery and House (1968), Auer (1968) and Weymann and Williams (1969) have considered the effects of natural and Doppler broadening with isotropic scattering by using Hummer's (1969) velocity-dependent redistribution function, and found that the emergent line profiles from a differentially moving chromospheric type of atmosphere are significantly different from those calculated by using the approximation of complete redistribution, and that these show significant emission peaks. However, Magnan (1974) explained these emission peaks on the basis

Astrophysics and Space Science **58** (1978) 189–205.

that Cannon and Vardavas (1974) selected a wrong frame of reference and correctly pointed out that in a differentially moving medium the averaging of the redistribution must be done in the local frame of reference. Vardavas (1976a) calculated the line profiles from moving medium using $R_{\mathrm{I,II,III}}$ functions (for notation see Hummer, 1962) and again found substantial differences between the lines calculated by complete redistribution and those by partial redistribution. Shine *et al.* (1975) and Milkey *et al.* (1975) have shown that there is a marked improvement in the understanding of the centre-to-limb variation of the solar Ca II H and K lines when the assumption of complete redistribution is replaced by partial redistribution.

Mihalas *et al.* (1976) have made use of the averaged redistribution functions and electron scattering in calculating the emergent line profiles in a comoving frame of reference and found differences from the lines calculated with complete frequency redistribution due to electron scattering, while Hamann and Kudritzki (1977), having made calculations in a comoving frame for the function $R_{\mathrm{I-A}}$, found that the difference between the two cases is very small. In most of the cases there is evidence that large differences exist between the lines calculated by use of the approximation of complete redistribution and those calculated by partial distribution.

Therefore, it is quite important to see the nature of the effects in various circumstances that the different redistribution functions would have on the formation of spectral lines in moving media. In this series of papers we shall try to solve the line transfer with partial redistribution in static and expanding spherical media. In the present paper we shall formulate the solution of line transfer with partial redistribution for an arbitrary – that is, either stationary or moving – media in the framework of the discrete space theory. We shall formulate the solution of the transfer equations in detail for partial redistribution as these are different from those given in Grant and Peraiah (1972) and Peraiah and Grant (1973) – henceforward referred to as GP and PG, respectively – and this solution can be used in a medium with or without velocities in the rest frame of the star. In Section 2, the solution of the line transfer with partial redistribution is presented and in Section 3 the results are discussed.

2. Solution of the Radiative Transfer Equation with Partial Redistribution

The equation of line transfer for a two-level atom in spherical symmetry is written as

$$\mu \frac{\partial I(x, \mu, r)}{\partial r} + \frac{1 - \mu^2}{r} \frac{\partial I(x, \mu, r)}{\partial \mu} = \\ = K_l[\beta + \phi(x, \mu, r)][S(x, \mu, r) - I(x, \mu, r)] \tag{1}$$

and for the opposite-directed beam,

$$-\mu \frac{\partial I(x, -\mu, r)}{\partial r} - \frac{1 - \mu^2}{r} \frac{\partial I(x, -\mu, r)}{\partial \mu} = \\ = K_l[\beta + \phi(x, -\mu, r)][S(x, -\mu, r) - I(x, -\mu, r)] \tag{2}$$

where $I(x, \mu, r)$ is the specific intensity at an angle $\cos^{-1}\mu$ ($\mu \in (0, 1)$) at the radial point r and frequency $x\,(=(\nu - \nu_0)/\Delta s$, where Δs is some standard frequency interval). The source function $S(x, \pm\mu, r)$ is given by

$$S(x, \pm\mu, r) = \frac{\phi(x, \pm\mu, r)S_l(x, \pm\mu, r) + \beta S_c(r)}{\phi(x, \pm\mu, r) + \beta}, \tag{3}$$

and the line source function $S_l(x, \pm\mu, r)$ is given by

$$S_l(x, \pm\mu, r) = \frac{(1 - \epsilon)}{\phi(x, \pm\mu, r)} \int_{-\infty}^{+\infty} dx' \int_{-1}^{+1} R(x, \pm\mu; x', \mu') \times \\ \times I(x', \mu')\, d\mu' + \varepsilon B(r), \tag{4}$$

where ε is the probability per scatter that a photon will be destroyed by collisional de-excitation; β is the ratio K_c/K_l of opacity due to continuous absorption per unit interval of x to that in the line; S_c and B are the continuum source function and Planck function, respectively; and $\phi(x, \pm\mu, r)$ and $R(x, \pm\mu; x', \mu')$ are the profile and partial redistribution functions. In this paper we shall consider two cases of angle-dependent and angle-averaged redistribution functions corresponding to (1) zero natural line width (R_{I}) and (2) radiation damping with coherence in the atom rest frame (R_{II}) given by (Hummer, 1962; Mihalas, 1970)

$$R_{\mathrm{I-AD}}(x, \mathbf{n}; x', \mathbf{n}') = \frac{g(\mathbf{n}, \mathbf{n}')}{4\pi^2 \sin^2\Theta} \exp\left\{-x'^2 - (x - x'\cos\Theta)^2 \operatorname{cosec}^2\Theta\right\}, \tag{5}$$

$$R_{\mathrm{II-AD}}(x, \mathbf{n}; x', \mathbf{n}') = \frac{g(\mathbf{n}, \mathbf{n}')}{4\pi^2 \sin^2\Theta} \exp\left\{-\left(\frac{x - x'}{2}\right)^2 \operatorname{cosec}^2(\Theta/2)\right\} \\ \times H\left(a \sec\frac{\Theta}{2}, \frac{x + x'}{2} \sec\frac{\Theta}{2}\right), \tag{6}$$

where the well-known Voigt function is given by

$$H(a, u) = \frac{a}{\pi} \int_{-\infty}^{+\infty} \frac{e^{-y^2}}{(u - y)^2 + a^2}\, dy, \tag{7}$$

in which the direction vectors $\mathbf{n}$ and $\mathbf{n}'$ correspond to the absorbed and emitted photon, Θ is the angle between these two vectors and a is the damping constant. We shall consider isotropic scattering, and in this case the quantity $g(\mathbf{n}, \mathbf{n}')$ is given by

$$g(\mathbf{n}, \mathbf{n}') = 1/4\pi. \tag{8}$$

The averaged functions are given (see Hummer, 1962) by

$$R_{\mathrm{I-A}}(x, x') = \tfrac{1}{2}\mathrm{erfc}(|\bar{x}|), \tag{9}$$

where

$$\operatorname{erfc}(x) = \frac{2}{\sqrt{\pi}} \int_x^\infty e^{-t^2}\, dt \tag{10}$$

and

$$R_{\text{II-A}}(x, x') = \frac{1}{\pi^{3/2}} \int_{\frac{1}{2}|\bar{x}-\underline{x}|}^\infty e^{-u^2} \left\{ \tan^{-1}\left(\frac{\underline{x}+u}{a}\right) - \tan^{-1}\left(\frac{\bar{x}-u}{a}\right) \right\} du, \tag{11}$$

where $\bar{x}$ and $\underline{x}$ are the larger and smaller values of x and x', respectively. The profile function ϕ is given by

$$4\pi \int\int R(\nu, \mathbf{n}; \nu', \mathbf{n}')\, d\nu'\, d\Omega' = \phi(\nu). \tag{12}$$

For various symmetry relations of the redistribution functions, see Hummer (1962) and Milkey *et al.* (1975).

Equations (1) and (2) are solved by using the source functions defined in Equations (3) and (4) together with the redistribution functions (5), (6), (9) and (11) and following the procedure of integration described in PG and GP. This gives us

$$\begin{aligned} &\mathbf{M}_m(\mathbf{u}^+_{i,n+1} - \mathbf{u}^+_{i,n}) + \varrho_c(\mathbf{\Lambda}^+_m \mathbf{u}^+_{i,n+\frac{1}{2}} + \mathbf{\Lambda}^-_m \mathbf{u}^-_{i,n+\frac{1}{2}}) + \tau_{n+\frac{1}{2}}(\beta + \boldsymbol{\phi}^+_{m,i})\mathbf{u}^+_{i,n+\frac{1}{2}} = \\ &\quad = \tau_{n+\frac{1}{2}}(\varrho\beta + \varepsilon\boldsymbol{\phi}^+_{m,i})_{n+\frac{1}{2}} \mathbf{B}'_{n+\frac{1}{2}} + \tfrac{1}{2}\tau_{n+\frac{1}{2}}(1-\varepsilon) \times \\ &\qquad \times (\mathbf{R}^{+\,+}_{i,i',n+\frac{1}{2}} \mathbf{a}^{+\,+}_{\frac{1}{2}i',n+\frac{1}{2}} \mathbf{c}\mathbf{u}^+_{i',n+\frac{1}{2}} + \mathbf{R}^{+\,-}_{i,i',n+\frac{1}{2}} \mathbf{a}^{+\,-}_{i',n+\frac{1}{2}} \mathbf{c}\mathbf{u}^-_{i',n+\frac{1}{2}}). \end{aligned} \tag{13}$$

Similarly, for the opposite-directed beam,

$$\begin{aligned} &\mathbf{M}_m(\mathbf{u}^-_{i,n} - \mathbf{u}^-_{i,n+1}) - \varrho_c(\mathbf{\Lambda}^+_m \mathbf{u}^-_{i,n+\frac{1}{2}} + \mathbf{\Lambda}^-_m \mathbf{u}^+_{i,n+\frac{1}{2}}) + \tau_{n+\frac{1}{2}}(\beta + \boldsymbol{\phi}^-_{m,i})_{n+\frac{1}{2}} \mathbf{u}^-_{i,n+\frac{1}{2}} = \\ &\quad = \tau_{n+\frac{1}{2}}(\varrho\beta + \in\boldsymbol{\phi}^-_m)\mathbf{B}'_{n+\frac{1}{2}} + \tfrac{1}{2}\tau_{n+\frac{1}{2}}(1-\varepsilon) \times \\ &\qquad \times (\mathbf{R}^{-\,+}_{i,i',n+\frac{1}{2}} \mathbf{a}^{-\,+}_{i',n+\frac{1}{2}}\, \mathbf{c}\mathbf{u}^+_{i',n+\frac{1}{2}} + \mathbf{R}^{-\,-}_{i,i',n+\frac{1}{2}} \mathbf{a}^{-\,-}_{i',n+\frac{1}{2}} \mathbf{c}\mathbf{u}_{n+i^-,n\frac{1}{2}}), \end{aligned} \tag{14}$$

where

$$\begin{aligned} \mathbf{u}^+_{i,n+1} &= 4\pi r^2_{n+1} \mathbf{I}(x_i, +\mu_m, r_{n+1}), \\ \boldsymbol{\phi}^+_{m,i,n+\frac{1}{2}} &= \boldsymbol{\phi}(x_i, +\mu_m, r_{n+\frac{1}{2}}), \\ \mathbf{R}^{+\,+}_{j,i'.n+\frac{1}{2}} &= \mathbf{R}(x_i, +\mu_m; x_{i'}, +\mu'_m; r_{n+\frac{1}{2}}); \end{aligned}$$

the $\mathbf{\Lambda}$'s are curvature matrices; ϱ_c is the curvature factor; and

$$\mathbf{B}'_{n+\frac{1}{2}} = 4\pi r^2{}_{n+\frac{1}{2}} B\nu, \qquad \mathbf{c} = [C_m \delta_{mk}],\ \mathbf{M}_m = [\mu_m \delta_{mk}];$$

in which the μ's and c's are the roots and weights of the angle quadrature. The quantities ϕ^-, $R^{-\,+}$, etc., are to be similarly understood. The index $n + \frac{1}{2}$ refers to the average over the shell with boundaries r_n and r_{n+1}, and i and i' are the indices corresponding to the frequencies of the incident and scattered photons.

We can define the coefficients $W_{k;n+\frac{1}{2}}$ as

$$(\phi_i W_k) = a_{i,n+\frac{1}{2}} c_j, \tag{15}$$

where the subscript k is

$$(i,j) \equiv k \equiv j + (i-1)J,\ 1 \leqslant k \leqslant K = IJ;$$

with I and J being the total number of frequency and angle points, respectively. The a's are as defined in Equation (23).

Let

$$\begin{aligned} \mathbf{u}_n^+ &= [\mathbf{u}_{1,n}^+, \mathbf{u}_{2,n}^+, \mathbf{u}_{3,n}^+, \ldots, \mathbf{u}_{I,n}^+]^T, \\ \mathbf{\Phi}_{n+\frac{1}{2}}^- &= [\mathbf{\Phi}_{kk'}^+]_{n+\frac{1}{2}} = (\beta + \phi_k^+)_{n+\frac{1}{2}} \delta_{kk'}, \\ \mathbf{s}_{n+\frac{1}{2}}^+ &= (\varrho\beta + \varepsilon\phi_k^+)_{n+\frac{1}{2}} B'_{n+\frac{1}{2}} \delta_{kk'}, \end{aligned} \tag{16}$$

where T denotes transpose, and rewrite Equations (13) and (14) as

$$\begin{aligned} &\mathbf{M}[\mathbf{u}_{n+1}^+ - \mathbf{u}_n^+] + \varrho_c[\mathbf{\Lambda}^+ \mathbf{u}_{n+\frac{1}{2}}^+ + \mathbf{\Lambda}\mathbf{u}_{n+\frac{1}{2}}^-] + \tau_{n+\frac{1}{2}} \mathbf{\Phi}_{n+\frac{1}{2}}^+ \mathbf{u}_{n+\frac{1}{2}}^+ = \\ &\quad = \tau_{n+\frac{1}{2}} \mathbf{s}_{n+\frac{1}{2}}^+ + \tfrac{1}{2}(1-\varepsilon)\tau_{n+\frac{1}{2}} [\mathbf{R}^{++}\mathbf{W}^{++}\mathbf{u}^+ + \mathbf{R}^{+-}\mathbf{W}^{+-}\mathbf{u}^-]_{n+\frac{1}{2}} \end{aligned} \tag{17}$$

and

$$\begin{aligned} &\mathbf{M}[\mathbf{u}_n^- - \mathbf{u}_{n+1}^-] - \varrho_c[\mathbf{\Lambda}^+ \mathbf{u}_{n+\frac{1}{2}}^- + \mathbf{\Lambda}^- \mathbf{u}_{n+\frac{1}{2}}^+] + \tau_{n+\frac{1}{2}} \mathbf{\Phi}_{n+\frac{1}{2}}^- \mathbf{u}_{n+\frac{1}{2}}^- = \\ &\quad = \tau_{n+\frac{1}{2}} \mathbf{s}_{n+\frac{1}{2}}^- + \tfrac{1}{2}(1-\varepsilon)\tau_{n+\frac{1}{2}} [\mathbf{R}^{-+}\mathbf{W}^{-+}\mathbf{u}^+ + \mathbf{R}^{--}\mathbf{W}^{--}\mathbf{u}^-]_{n+\frac{1}{2}}. \end{aligned} \tag{18}$$

The average intensities $\mathbf{u}_{n+\frac{1}{2}}^-$ in the above equations are replaced by the relations (2.23) of GP and by comparing the resulting set of equations with those in the canonical form (2.15) of PG we obtain two pairs of reflection and transmission operators, together with the source vectors; these are given in the Appendix. These operators describe the radiation field in a moving medium and, therefore, all four redistribution functions $R(x, +\mu; x', \mu')\,(=R^{++})$, $R(x, +\mu; x', -\mu)(=R^{+-})$ $R(x, -\mu; x', +\mu')$ $(=R^{-+})$ and $R(x, -\mu; x', -\mu')(=R^{--})$ are not equal and have to be calculated at each radial point of the medium. However, if the medium is static and partial redistribution is considered, then, by the symmetry relations (Hummer, 1962), we have

$$\begin{aligned} R(x, +\mu; x', +\mu') &= R(x, -\mu; x', -\mu'); \qquad R^{++} = R^{--} \\ R(x, +\mu; x'; -\mu') &= R(x, -\mu; x', +\mu'); \qquad R^{+-} = R^{-+}. \end{aligned}$$

Furthermore, if we consider a static medium with complete redistribution, then all four redistribution functions that evaluate the scattering integral reduce to approximately $\phi\phi^T$, where ϕ is the profile function and T is the transpose of the vector. Consequently, the form of the quantities $\mathbf{Z}_+$, $\mathbf{Z}_-$, $\mathbf{Y}_+$, $\mathbf{Y}_-$, etc., given in the Appendix will be reduced to those given in GP.

To obtain a stable solution one must choose an optical depth $\tau_{n+\frac{1}{2}}$ in each cell,

given by

$$\tau_{n+\frac{1}{2}} \leqslant \tau_{\text{crit}} = \min_k \left| \frac{\mu_k \pm \frac{1}{2}\varrho_c \Lambda^+_{kk}}{\frac{1}{2}(\Phi^+_k - \frac{\sigma}{2} R^{++}_{kk} W^{++}_{kk})} \right| \tag{19}$$

for the diagonal elements of the matrices $\mathbf{\Delta}^+$ and $\mathbf{\Delta}^-$ given in the Appendix, and for the off-diagonal element we must have

$$(\varrho_c/\tau)_{n+\frac{1}{2}} < \min_k \left[\min_{k=k'\pm 1} \left| \frac{\frac{1}{2}\sigma R_{kk'} W_{kk'}}{\Lambda^+_{kk'}} \right| \right]. \tag{20}$$

Condition (20) is difficult to satisfy, which imposes a severe restriction on the size of the curvature factor to be used in each cell to obtain non-negative r and t matrices. From the inequalities set out in (19) and (20) above, it is clear that the medium of interest should be divided into a number of shells and relations (5.1) to (5.4) of PG should be used to calculate the diffuse radiation field at any point in the medium. However, it is time consuming to use a large number of shells and subdivide each shell so that the curvature factor ϱ_c is small enough to facilitate the use of the doubling algorithm described in Peraiah (1975) and the star algorithm of Grant and Hunt (1969a,b).

If the shell is halved p times, the star algorithm is repeated p times, and in this event the curvature factor ϱ_{ss} and the optical depth τ_{ss} for the subshell are given in terms of ϱ_s and τ_s of the shell

$$\begin{aligned} &\varrho_{ss} \approx \varrho_s 2^{-p}/[1 - \varrho_s(2^{-1} - 2^{-p})], \\ &\tau_{ss} = \tau_s 2^{-p}, \\ &r^2 = R^2[1 - \varrho_s(K + \tfrac{1}{2}) + \tfrac{1}{3}\varrho_s^2(K^2 + \tfrac{1}{2}k + \tfrac{1}{4})]; \end{aligned} \tag{21}$$

where ϱ_{ss} corresponds to a subshell approximately midway in the shell and ϱ_s is the curvature factor for the whole shell, defined as

$$\varrho_s = \Delta r/r_{\text{out}}, \tag{22}$$

τ_{ss} being derived on the assumption that the optical depth is uniform in the whole shell. ϱ_{ss} is taken to be the mean value for all subshells, which introduces error, and to reduce this error one must divide the shell into finer subshells that are small enough not to introduce serious errors. $\bar{r}$ is the mean radius of the subshell; R is the outer radius of the shell in terms of the inner radius of the medium: and $K = 2^{-1} - 2^{-p}$. The relations set out in (21) are derived on the basis of Equation (30) of Grant (1963).

To conserve flux, one must ensure that the scattering integral given in Equation (4), and the corresponding discrete equivalent given in the last brackets of Equations (13), (14), (17) and (18), are calculated exactly. For this purpose, the redistribution functions R^{++}, R^{+-}, etc., must be normalized to the machine accuracy so that, when we have pure scattering in the medium, conservation of flux can be checked easily (see PG).

This can be achieved through the identity

$$\tfrac{1}{2}\sum_{P=1}^{K}\sum_{Q=1}^{K}(R_{PQ}^{++}W_P^{+}W_Q^{+} + R_{PQ}^{-+}W_P^{-}W_Q^{+}) = 1, \tag{23}$$

where

$$W_{P,Q} = a_i c_j,\ a_i = \frac{A_i R_{PQ}}{\sum_{P,Q=1}^{K} R_{PQ} A_i c_j} \quad \text{and} \quad (P, Q) \equiv j + (i + i)J;$$

and also by relation (4.3) of PG.

For the case $\varepsilon = 0$, the program has been checked and it is found that the flux is conserved to the machine accuracy. In the next section we shall describe the results for a static medium.

3. Results and Discussion

There are a large number of parameters for which the lines can be calculated. Consequently, we have chosen some representative values of these parameters to show how the method works and to portray the differences between plane-parallel (PP) and spherically symmetric (SS) geometries using the angle-dependent and angle-averaged redistribution functions. It is of considerable importance to calculate the redistribution functions accurately. We have followed the procedures described in Adams *et al.* (1971) and Milkey *et al.* (1975) in calculating the angle-averaged and angle-dependent functions, respectively. Voigt profiles are calculated by use of the algorithm of Baschek *et al.* (1966). The damping constant is set equal to 0.5×10^{-3} and a total optical depth T equal to 10^3 has been used throughout the calculations, assuming isotropic scattering.

The algorithm can easily be tested for accuracy and stability when an atmosphere which can neither create nor destroy photons is considered, and in this situation the flux of radiation that is incident on the two boundaries of the atmosphere must balance the flux that emerges. For this purpose we have treated a pure scattering media with $\varepsilon = 0 = \beta$ and $B/A = 1$ and 2 for PP and SS geometries, respectively. The boundary conditions for this case (case 1) are

$$u_1^{+}(x_i, \tau = 0, \mu_j) = 0$$

and (24)

$$u_{N+1}^{-}(x_i, \tau = T, \mu_j) = 1.$$

We have also considered another case where there is some emission in the line with $\varepsilon = 10^{-4}$, $\beta = 0$ and $B/A = 1$, 2 and 10 and the boundary conditions for this case (case 2) are

$$u_1{}^{+}(x_i, \tau = 0, \mu_j) = u_{N+1}^{-}(x_i, \tau = T, \mu_j) = 0, \tag{25}$$

where N is the total number of shells into which the medium has been divided (see

Equations (19) and (20) for reasons). We have not included any continuum emission as we are only testing the method for its stability and properties of flux conservation when PRD functions are treated.

The quantity $B'(\bar{r})$ in Equations (16) is set equal to unity so that

$$B(\bar{r}) = \frac{1}{4\pi\bar{r}^2} \tag{26}$$

for the case 2.

The frequency- and angle-independent source function $S_l(\tau_n)$ at the boundary of

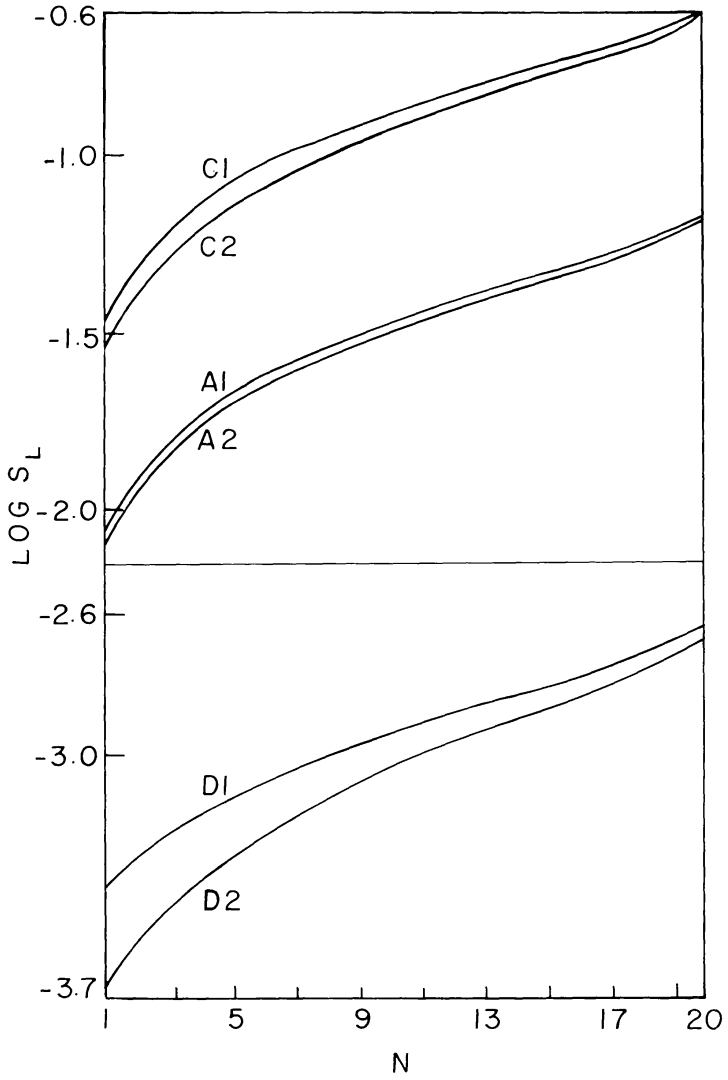

Fig. 1. Frequency-independent line source function log S_l (see Equation (27)) is plotted against the shell number N, for case 1 and for the redistribution function R_{II}. All shells are of equal optical depth. Numerals represent the quantity B/A, the ratio of outer to inner radius and the letters C, A and D represent complete redistribution, angle-averaged and angle-dependent redistribution functions, respectively.

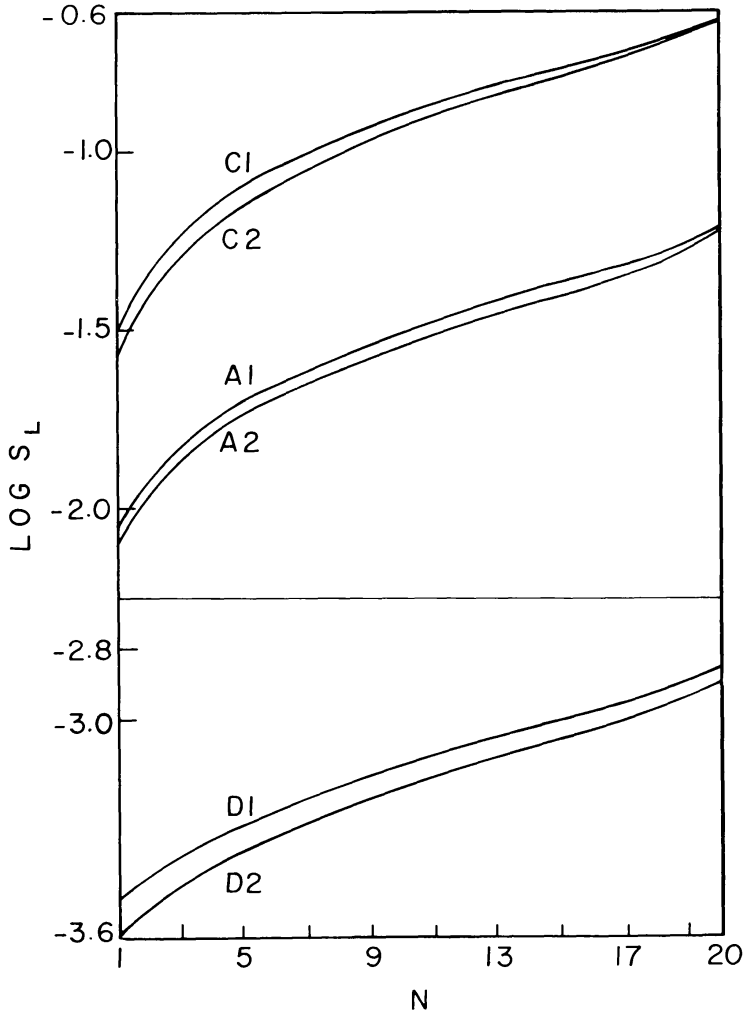

Fig. 2. Frequency-independent line source functions log S_l is plotted against shell number N for the redistribution function R_{II}.

each shell, and the monochromatic emergent flux F_x, are calculated by the relations

$$S_l(\tau_n) = \sum_{i=1}^{I} \sum_{j=1}^{J} S(x_i, \mu_j, \tau_n) A_i c_j \tag{27}$$

and

$$F_{x_i} = \left(\frac{A}{B}\right)^2 \sum_{j=1}^{J} u_1^-(x_i, \mu_j, \tau = 0) c_j \mu_j . \tag{28}$$

We have employed 20 frequency points and 4 angle points, and the medium has been divided into 20 shells, each of equal optical and geometrical thicknesses. The program has been checked for flux conservation in the purely scattering medium of case 1 and it is found that it satisfies the printed 8 digits.

The frequency-independent source functions S_l (Equation (27)) corresponding to the lines with zero natural line width (R_I) and those with radiation damping with

coherence in the atom rest frame are respectively plotted in Figures 1 and 2 against the shell number N for the medium with pure scattering ($\varepsilon = 0, \beta = 0$). The letters C, A and D represent complete redistribution, angle-averaged and angle-dependent redistribution functions respectively, and the associated numerals correspond to the ratio B/A ($B/A = 1$ for PP and $B/A > 1$ for SS geometries). The shell numbers $N = 1$ and $N = 20$ refer to outer ($\tau = 0$) and inner ($\tau = T$) boundaries, respectively. The source functions reach maximum values at $N = 20$ and minimum values at $N = 1$ both in PP and SS geometries for all the scattering functions. When there are no internal sources ($\varepsilon = 0, \beta = 0$), and scattering is the only physical process in the medium, the source function will be maximum at the boundary of incident radiation (see Equation (24), $\tau = T$) and will gradually reduce to its minimum at the top of the medium ($\tau = 0$) where no incident radiation is given. The spherical values lie below their plane-parallel counterparts in all three cases of the scattering functions (see GP; Kunasz and Hummer, 1974; Vardavas, 1976b). The source functions in PP and SS

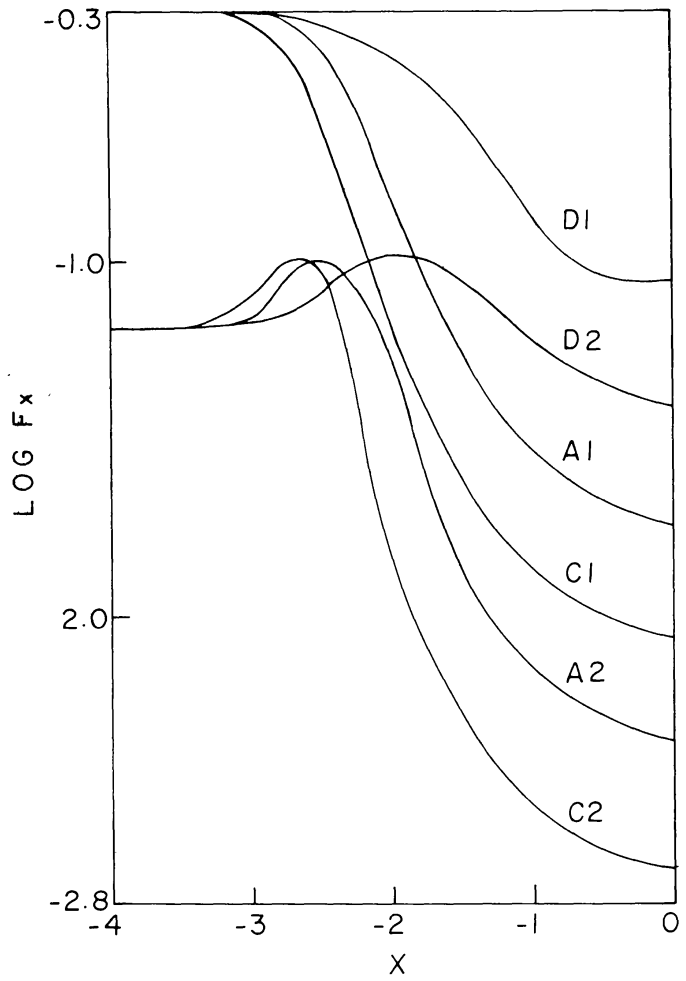

Fig. 3. Emergent line profiles corresponding to the line source function given in Figure 1 are given in terms of log F_x versus x.

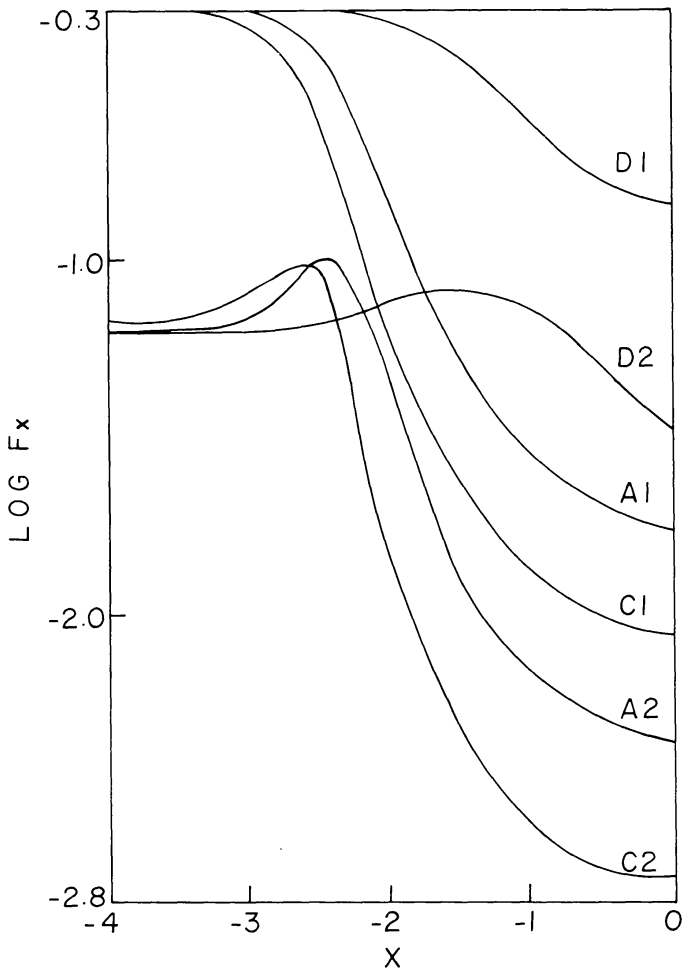

Fig. 4. Same as those in Figure 3 but corresponding to the line source function given in Figure 2.

geometries tend to converge as they reach the bottom of the atmosphere in the case of CRD and angle-averaged redistribution functions, whereas those corresponding to the angle-dependent redistribution functions show noticeable differences. These differences tend to increase towards the top of the atmosphere ($\tau = 0$), and the source functions corresponding to the angle-dependent redistribution functions in SS geometry fall off more rapidly than those corresponding to either CRD or angle-averaged redistribution. In spherical media, the ray continuously changes its angle with the radius vector, and when the scattering of radiation is treated by an angle-dependent redistribution function these two effects are added, thus enhancing the differences between the values of PP and SS geometries. Therefore, substantial differences could exist between the emergent fluxes calculated by the PP approximation and those calculated by the SS approximation when the angle-dependent scattering functions are used. This is particularly true in the case of a moving medium where the velocity vector is properly taken into account. The emergent flux profiles (Equation (28)) corresponding to the lines with zero natural line width (R_{I}) and those with radiation

damping with coherence in the atom rest frame (R_{II}) are respectively plotted in Figures 3 and 4; the corresponding frequency-independent source functions are described in Figures 1 and 2. The lines in SS geometry lie below their counterparts in PP geometry for all scattering functions (see GP; Kunasz and Hummer, 1974; Vardavas, 1976b). The wings of the lines in SS are reduced by an almost constant factor from those in PP geometry, but the cores differ substantially from each other. The lines formed in SS geometry show small wing emission and are broader than those formed in PP geometry. The lines corresponding to R_{I-AD} and R_{II-AD} (AD representing the angle-dependent functions) show more emission in their line wings than those corresponding to the other redistribution functions, and this emission spreads more towards the centre of the line for lines formed by the R_{II} function than for those formed by the R_I function. The curvature effects give rise to substantial differences between the lines formed in SS and PP geometries and the forward-peaking effect changes mainly the shapes of the lines formed by the R_{I-AD} and R_{II-AD} functions. The joint effect of atmospheric curvature and physical scattering is responsible for this emission in the wings, and more photons escape through the wings. The lines in SS geometry are broader, and those formed by PRD functions have more photons scattered into their cores than those formed by CRD, and this is more so for R_{I-AD} and R_{II-AD}.

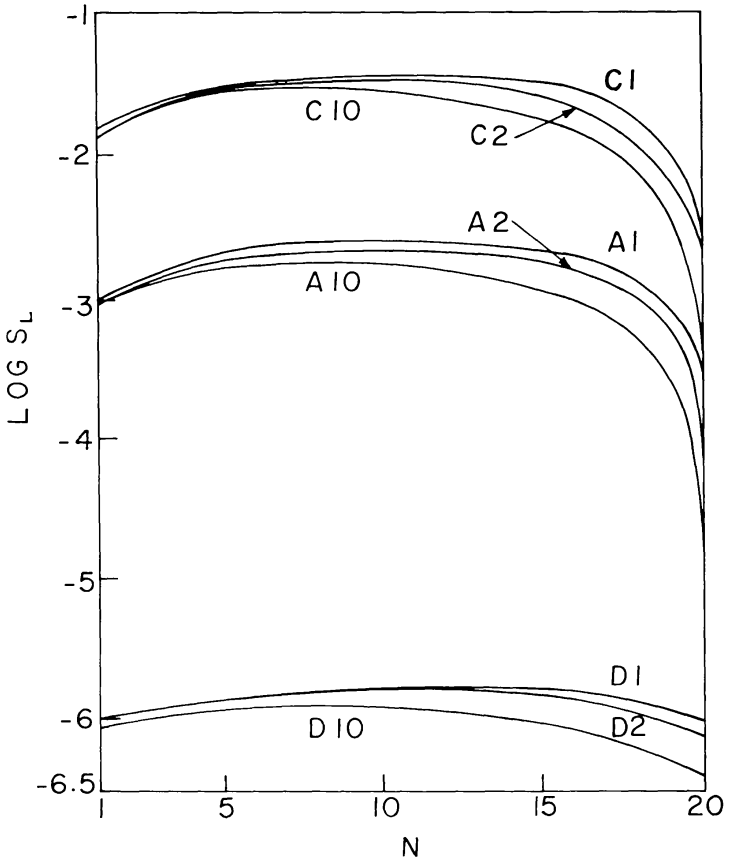

Fig. 5. Frequency-independent line source functions S_l for case 2 and R_I.

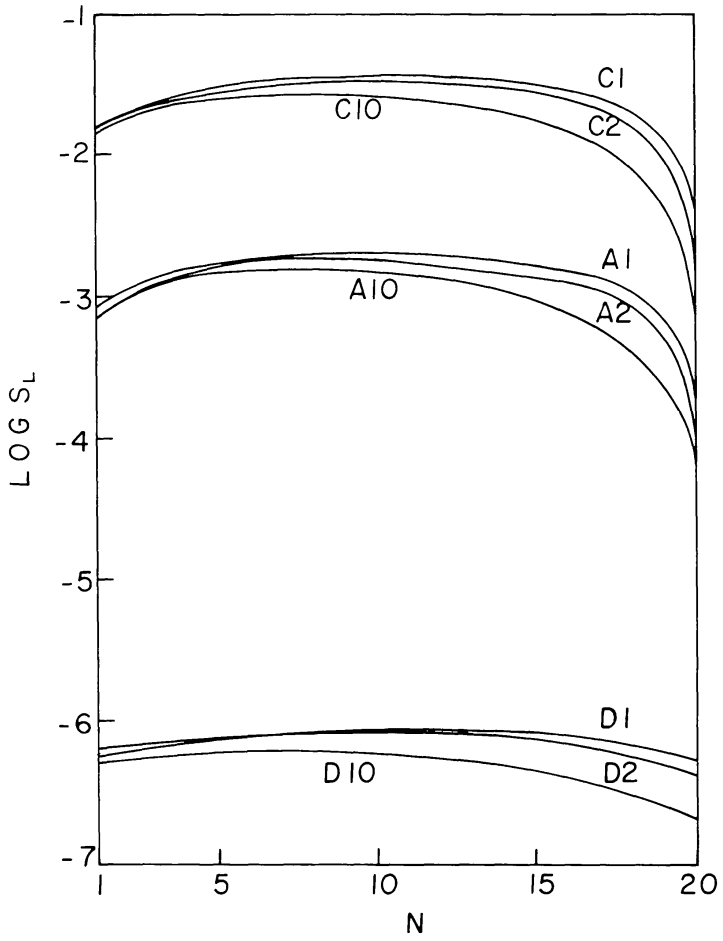

Fig. 6. Frequency-independent line source functions S_l for case 2 and R_I.

In Figures 5 and 6 the source functions corresponding respectively to the scattering functions R_I and R_{II} are described for the medium of case 2 with line emission ($\varepsilon = 10^{-4}, \beta = 0$) for $B/A = 1$, 2 and 10. The source functions of SS geometry lie below those of PP geometry, similar to the purely scattering medium of case 1. For most of the atmosphere, the source functions for all cases are constant and fall off sharply at the boundary $N = 20$ ($\tau = T$) except those corresponding to the angle-dependent redistribution functions. No incident radiation has been given at either boundary (see the boundary condition given in (25)) and therefore the source functions are smaller at the boundaries. As the medium is assumed to the homogeneous (and therefore constant ε), we see that the source function becomes almost constant inside the atmosphere. However, the source functions corresponding to R_{I-AD} and R_{II-AD} do not fall off as rapidly as those of the angle-averaged functions because the curvature factor $\varrho_c (= \Delta r/r$, where Δr is the geometrical thickness and r is the outer radius of the shell) at the inner boundary (nearer the centre of the star) is maximum and this, coupled with the angle-dependence of the scattering functions, increases the mean

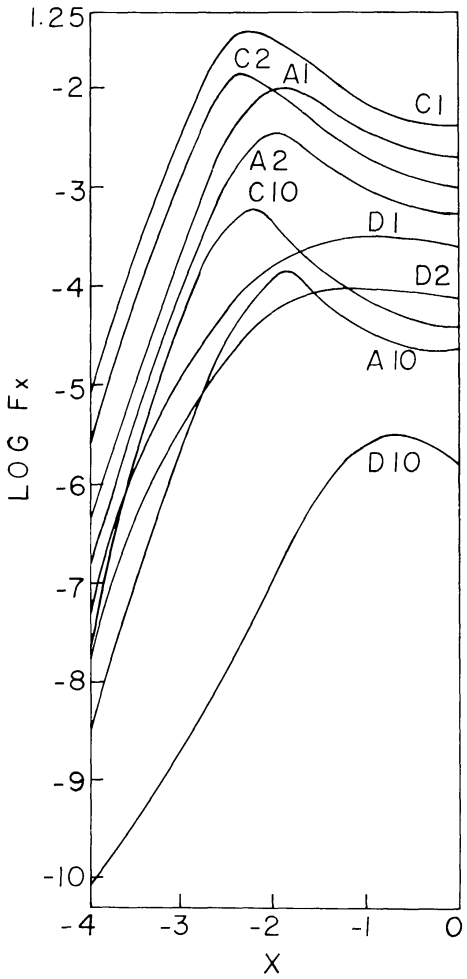

Fig. 7. Emergent line profiles corresponding to the source functions given in Figure 5.

intensity and hence the source function. The corresponding emergent flux profiles to the source functions given in Figures 5 and 6 are plotted in Figures 7 and 8, respectively. These profiles differ substantially from those given in Figures 3 and 4 because the latter are formed by a purely scattering medium and the former are the emergent profiles from a medium with line emission. In the absence of continuous emission, the line emission becomes more prominent ($\varepsilon = 10^{-4}, \beta = 0$) and therefore we notice a large emission in the wings and absorption in the cores. This is true in all cases except in the lines formed by $R_{\text{I-AD}}$ and $R_{\text{II-AD}}$ in which there is no self-absorption in PP geometry, but as the ratio B/A increases from 1 to 10, the self-absorption develops gradually for $R_{\text{I-AD}}$ and higher geometrical extensions are required before any self-absorption is noticed. The wings of the profiles corresponding to R_{I} drop sharply, whereas those corresponding to R_{II} become broader; also, lines in the latter case have more photons scattered into their wings than those in the former case.

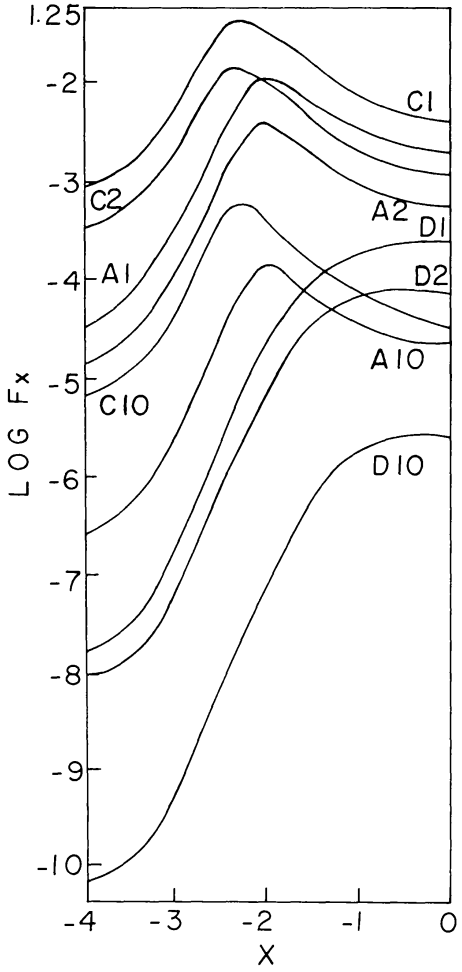

Fig. 8. Emergent line profiles corresponding to the source functions given in Figure 6.

4. Conclusions

Large differences between the lines formed by CRD and those formed by PRD are found to exist, and these differences continue to persist in either geometry although in SS geometry the peaking effect further enhances the differences. In particular, the lines calculated with the angle-dependent PRD functions show marked differences, a fact that must be taken into consideration when the lines are calculated in a differentially moving medium.

Acknowledgements

This work has been performed as part of the Sonderforschungsbereich 132 'Theoretische und Praktische Stellarastronomie' which is sponsored by the Deutsche Forschungsgemeinschaft.

Appendix

The cell operators are

$$\mathbf{t}(n+1,n) = \mathbf{G}^{+-}[\mathbf{\Delta}^{+}\mathbf{A} + \mathbf{g}^{+-}\mathbf{g}^{-+}],$$
$$\mathbf{t}(n,n+1) = \mathbf{G}^{-+}[\mathbf{A}^{-}\mathbf{D} + \mathbf{g}^{-+}\mathbf{g}^{+-}],$$
$$\mathbf{r}(n+1,n) = \mathbf{G}^{-+}\mathbf{g}^{-+}[\mathbf{I} + \mathbf{\Delta}^{+}\mathbf{A}],$$
$$\mathbf{r}(n,n+1) = \mathbf{G}^{+-}\mathbf{g}^{+-}[\mathbf{I} + \mathbf{\Delta}^{-}\mathbf{D}]$$

and the cell source vectors are

$$\mathbf{\Sigma}^{+}_{n+\frac{1}{2}} = \mathbf{G}^{+-}[\mathbf{\Delta}^{+}\mathbf{s}^{+}_{n+\frac{1}{2}} + \mathbf{g}^{+-}\mathbf{\Delta}^{-}\mathbf{s}^{-}_{n+\frac{1}{2}}]\tau_{n+\frac{1}{2}}$$

and

$$\mathbf{\Sigma}^{-}_{n+\frac{1}{2}} = \mathbf{G}^{-+}[\mathbf{\Delta}^{-}\mathbf{s}^{-}_{n+\frac{1}{2}} + \mathbf{g}^{-+}\mathbf{\Delta}^{+}\mathbf{s}^{+}_{n+\frac{1}{2}}]\tau_{n+\frac{1}{2}},$$

where

$$\mathbf{G}^{+-} = [\mathbf{I} - \mathbf{g}^{+-}\mathbf{g}^{-+}]^{-1},$$
$$\mathbf{G}^{-+} = [\mathbf{I} - \mathbf{g}^{-+}\mathbf{g}^{+-}]^{-1},$$
$$\mathbf{g}^{+-} = \tfrac{1}{2}\tau_{n+\frac{1}{2}}\mathbf{\Delta}^{+}\mathbf{Y}_{-},$$
$$\mathbf{g}^{-+} = \tfrac{1}{2}\tau_{n+\frac{1}{2}}\mathbf{\Delta}^{-}\mathbf{Y}_{+},$$
$$\mathbf{D} = \mathbf{M} - \tfrac{1}{2}\tau_{n+\frac{1}{2}}\mathbf{Z}_{-},$$
$$\mathbf{A} = \mathbf{M} - \tfrac{1}{2}\tau_{n+\frac{1}{2}}\mathbf{Z}_{+},$$
$$\mathbf{\Delta}^{+} = [\mathbf{M} + \tfrac{1}{2}\tau_{n+\frac{1}{2}}\mathbf{Z}_{+}]^{-1},$$
$$\mathbf{\Delta}^{-} = [\mathbf{M} + \tfrac{1}{2}\tau_{n+\frac{1}{2}}\mathbf{Z}_{-}],$$
$$\mathbf{Z}_{+} = \mathbf{\Phi}^{+}_{n+\frac{1}{2}} - \tfrac{1}{2}\sigma(\mathbf{R}^{++}\mathbf{W}^{++})_{n+\frac{1}{2}} + \varrho_c\mathbf{\Lambda}^{+}/\tau_{n+\frac{1}{2}},$$
$$\mathbf{Z}_{-} = \mathbf{\Phi}^{-}_{n+\frac{1}{2}} - \tfrac{1}{2}\sigma(\mathbf{R}^{--}\mathbf{W}^{--})_{n+\frac{1}{2}} - \varrho_c\mathbf{\Lambda}^{+}/\tau_{n+\frac{1}{2}},$$
$$\mathbf{Y}_{+} = (\varrho_c\mathbf{\Lambda}/\tau_{n+\frac{1}{2}}) + \tfrac{1}{2}\sigma(\mathbf{R}^{-+}W^{-+})_{n+\frac{1}{2}},$$
$$\mathbf{Y}_{-} = -(\varrho_c\mathbf{\Lambda}^{-}/\tau_{n+\frac{1}{2}}) + \tfrac{1}{2}\sigma(\mathbf{R}^{+-}\mathbf{W}^{+-})_{n+\frac{1}{2}},$$
$$\sigma = 1 - \varepsilon,$$

and $\mathbf{I}$ is the unitary matrix.

References

Adams, T. F., Hummer, D. G. and Rybicki, G. B.: 1971, *J. Quant. Spectr. Radiative Transfer* **11**, 1365.

Auer, L. H.: 1968, *Astrophys. J.* **153**, 783.

Avery, L. W. and House, L. L.: 1968, *Astrophys. J.* **152**, 493.

Baschek, B., Holweger, H. and Traving, G.: 1966, *Abh. Hamb. Sternwarte* **8**, 26.

Cannon, C. J. and Vardavas, I. M.: 1974, *Astron. Astrophys.* **32**, 85.

Carlson, B. G.: 1963, in B. Alder, A. Fernbach and M. Rotenberg (eds), *Methods of Computational Physics*, Vol. 1, Academic Press, New York, p. 1.

Grant, I. P.: 1963, *Monthly Notices Roy. Astron. Soc.* **125**, 417.

Grant, I. P. and Hunt, G. E.: 1969a, *Proc. Roy. Soc.* **A313**, 183.

Grant, I. P. and Hunt, G. E.: 1969b, *Proc. Roy. Soc.* **A313**, 199.

Grant, I. P. and Peraiah, A.: 1972, *Monthly Notices Roy. Astron. Soc.* **160**, 239.

Hamann, W. R. and Kudritzki, R. P.: 1977, *Astron. Astrophys.* **54**, 525.

Hummer, D. G.: 1962, *Monthly Notices Roy. Astron. Soc.* **125**, 21.

Hummer, D. G.: 1968, *Monthly Notices Roy. Astron. Soc.* **141**, 479.
Hummer, D. G.: 1969, *Monthly Notices Roy. Astron. Soc.* **145**, 95.
Kunasz, P. B. and Hummer, D. G.: 1974, *Monthly Notices Roy. Astron. Soc.* **166**, 19.
Lathrop, K. D. and Carlson, B. G.: 1967, *J. Comp. Phys.* **2**, 173.
Magnan, C.: 1974, *Astron. Astrophys.* **35**, 233.
Mihalas, D.: 1970, *Stellar Atmospheres*, W. H. Freeman & Co., San Francisco.
Mihalas, D., Kunasz, P. B. and Hummer, D. G.: 1976 *Astrophys. J.* **210**, 419.
Milkey, R. W., Shine, R. A. and Mihalas, D.: 1975, *Astrophys. J.* **202**, 250.
Peraiah, A.: 1975, *Astron. Astrophys.* **40**, 75.
Peraiah, A. and Grant, I. P.: 1973, *J. Inst. Maths Applics.* **12**, 75.
Shine, R. A., Milkey, R. W. and Mihalas.: 1975, *Astrophys. J.* **199**, 724.
Vardavas, I. M., 1974, *J. Quant. Spectr. Radiative Transfer* **14** 909.
Vardavas, I. M.: 1976a, *J. Quant. Spectr. Radiative Transfer* **16**, 781.
Vardavas, I. M.: 1976b, *J. Quant. Spectr. Radiative Transfer* **16**, 901.
Weymann, R. J. and Williams, R. E.: 1969, *Astrophys. J.* **157**, 1201.